EROSION MODEL CALIBRATION WITH GENETIC ALGORITHM

__Joan A. R. BOULANGER__[1*] , Chong Y. WONG[1],

M S Amir ZAMBERI[2], S N Amira SHAFFEE[2], Zurita JOHAR[3] and Maharon JADID[3]

[1] CSIRO Mineral Resources, Clayton, Victoria 3169, AUSTRALIA

[2]Group Technical Solution Petronas, MALAYSIA

[3] Petronas Carigali Sdn Bhd, MALAYSIA

*Corresponding author, E-mail address: Joan.Boulanger@csiro.au

ABSTRACT

Phenomenological erosion models are calibrated against bench testing using genetic algorithms. The usage of genetic algorithms allows one to process the sand particles impacts raw data accumulating arbitrarily on the exposed surface of the target without assumptions on their trajectories. The erosion model functional is a classical one, responding to velocity and angle of impact, but augmented with a particle diameter dependency at the material level. Computational Fluid Dynamics (CFD) supplements the bench tests in capturing the particle impact events. The technique is robust in delivering accurate erosion models for two types of material of different ductility and two types of carrier for the sand, generating high- and low-Stokes number behaviours complicating the mix of impact events at every point of the target surface. From the range of slip velocities and the size distribution of the sand reproduced by the CFD simulations, the genetic algorithm recovers, against the bench testing data, typical observed response of erosion to dispersed velocity and size. From an engineering point of view, the developed erosion models may be the first ones incorporating dispersed diameter response at the material level as an extended functional from systematic bench test campaigns. The possibility of calibrating directly from the raw data paves the way to rapid accurate erosion model development based on tests in the low-Stokes regime that remove wall restitution uncertainties from the particle trajectories as well as on parts of involved geometries.

NOMENCLATURE

A,B,W,X,Y,ϕ empirical angular erosion function parameters
C cost function normalisation
K erosion constant
L characteristic length
P erosion ratio prediction
R erosion ratio measurement
St Stokes number
V bulk velocity
c subscript, critical quantity
d particle diameter. Subscript, dispersed material.
e erosion ratio
f angular erosion function
i subscript, summation index
n impact velocity exponent, erosion model parameter
m number of measurements
v impact velocity
Φ cost function
α impact angle
β cylindrical angular coordinate
ρ mass density
μ dynamic viscosity

INTRODUCTION

Erosion is a general concern of capital and operating cost as well as from an environmental and safety point of view across virtually all industries and infrastructures. Systematic scientific and engineering investigation is prevalent since, at least, the 30's, (Rosenberg, 1930).

To any practical end, the challenge is the availability of models able to predict the risk of failure of a facility from the operating conditions. A typical sector heavily exposed is the resource industry: oil & gas wells producing sand or slurry transport in the mineral refineries, but every process relying on the conveyance of particles is threatened by erosion.

Literature Review

Erosion is observed to be primarily dependent on dispersed particle impact angle and velocity, and models are traditionally built as a function of these variables (Finnie, 1960), (Elfeki and Tabakoff, 1987), (Chen et al., 2004). These are semi-empirical models which need to be calibrated for particular combinations of suspended particles and target surfaces from bench testing. These tests involve simple geometries in order to explicitly identify impact velocities and angles (Wong et al., 2012), (Wallace et al., 2004). Unfortunately, this involves assumptions and approximations on the particles' actual trajectories that are not necessarily verified (Wong et al., 2013). When fluid mechanics disturbs the expected impact rate, velocity, and angle distribution, the problem must be decomposed in order to keep an explicit relationship between local erosion and impact events for the purpose of erosion model calibration (Solnordal et al., 2013). This may not be tractable for arbitrary configurations. Furthermore, other aspects of the dispersed material properties cannot be taken into account, such as grain diameter or shape, or density distribution since a single point on the target indifferently accumulates erosion contributions from entities with different values for these properties. In particular, there is a long-standing research effort to understand and incorporate into models the effect of the particle size in a reliable manner both from a fundamental point of view and to increase the robustness of the models developed for engineering purposes.

Erosion models aiming at estimating the exposition to erosion of a whole facility part for a set of operating conditions traditionally include particle size effect in a crude way. For instance (Salama, 1998a), (Salama, 1998b) incorporated a linear dependency on the particle diameter that saturates beyond 400 μm. Size dependency can also be evaluated from curve fitting, such as (Jordan, 1998), who found a particle size exponent of 1.6 and admitted from the literature that this fit should be limited by a plateau when reaching the range of [150-300] μm. Some of these engineering models recognise particle size effect on erosion from a fluid mechanics point of view only, as the elbow penetration factor in (McLaury and Shirazi, 1999) which

attempts to capture the variation in the particle approach towards an elbow extrados for a range of elbow curvatures, and (Det Norske Veritas, 2007) which extends the concept to other piping components.

A significant number of erosion experiments are carried out in slurry pots in dense configuration, e.g. (Desale et al., 2009). In these conditions, particle size effect can be dominated by the inter-particle interaction and the carrier streamline deviations at the approach of the target. Desale et al. (2009) report that larger particles impart more erosion damage beyond an impact kinetic energy threshold indirectly linked to their size, whereas below it, the wear is associated with abrasion. Lyon et al., (1991) highlight that erosion rate changes little with particle size larger than 500 μm, is proportional to impact kinetic energy in the range 100-500 μm and relies on a different mechanism of metal removal for particles below this range. Importantly, these latter experiments were done in low-concentration oil slurry and data treatment incorporated a correction for fluid mechanical effects in the neighbourhood of the target such that the size effect on erosion could be captured at the material level. On the other hand, authors suspected that the ability to clear the volume in front of the target surface after rebound was biased against small particles, which were strongly decelerated by the fluid, such that they were particularly prone to generate multiple impacts.

The fluid mechanics perturbing the particle trajectories near the impact may have a significant effect on the apparent particle diameter dependency of the erosion rate (Clark, 2002). In the low-Stokes number range, perturbed particle trajectories may create an acute apparent sensitivity, although seen in an air/slurry flow (Wong et al., 2014). The accepted interpretation is the deviation of small particles by the flow streamlines in the neighbourhood of the surface, (Laitone, 1979), but in some configurations the fluid mechanics effect is found to concentrate the impact of low-Stokes number particles on some areas (Schweitzer and Humphrey, 1988). The quantification of the apparent particle size effect due to fluid mechanics is difficult and may take a wide range of value (Wong et al., 2013). This apparent size effect induced by fluid mechanics is to be kept distinct from the erosion diameter dependency that is at the material level.

The effect of particle size on erosion is greater for brittle materials, (Stack and Pungiwat, 1999), and different responses to size have been observed including the existence of a maximum. This differs from most observations of an increasing function with a plateau asymptotic behaviour. It is hypothesized that, for erosion of brittle materials, cracks develop preferentially near the circumference of the contact area where the tensile stress is maximum (Finnie, 1960), and this is related to the size of the projectile. Comparing erosion of Pyrex as a brittle material, and aluminium as a ductile material, (Clark and Hartwitch, 2001) found that the particle size effect can be notably different with an existence or absence of a threshold in size to initiate damages, or a sharp or smooth sensitivity of wear to particle size.

Rationale

To deal with arbitrary configurations, the inverse problem of erosion model calibration must be made with techniques sophisticated enough to be able to treat the raw impingement data, since approach conditions may not be trivial to extract otherwise without simplifications. Additionally, when individual particles have different characteristics, e.g. size, the erosion at a given target location accumulates indistinctly the contribution of all the impacts. The inversion techniques must therefore be able to reconstruct this information in order to make these particle characteristics dependency variables of the erosion model. Extracting the erosion dependency on size at the material level is reckoned as a step forward to develop more accurate and robust erosion models. Another advantage

is the calibration of erosion models when bench tests are performed in the low-Stokes regime to minimise the uncertainties due to wall restitution as, in this regime, the trajectories are perturbed by the fluid in a non-obvious manner. Calibration on complex geometries exposed to erosion as field parts may also profit from this technique.

Objective

In this paper we demonstrate that genetic algorithms can be used affordably to calibrate erosion models. We highlight how such an approach allows remarkable flexibility in handling the raw inputs in terms of material loss distribution and dispersed trajectories such that no simplification or idealisation of the particles impact conditions is required.

Scope

The present contribution is limited to the presentation of the feasibility of using genetic algorithms for calibration of erosion models and the associated assets. Two target materials, varying in ductility behaviour, are considered: stainless steel and aluminium, allowing assessing the calibration of erosion models with significantly different response to the impact angle, which is the most mathematically involved function in the expression of these models. Two carriers are considered, water and air, at two bulk velocities, differing by one order of magnitude. These conditions create local particle Stokes numbers that differ by about three orders of magnitude. The erosion model expression to be calibrated is based on (Chen et al., 2004) but extended with a diameter dependency function whose shape is deduced from the general observations reported in the literature. One sand type is used. Material loss is measured from bench tests while particle impacts are collected by CFD. Demonstration of the calibration methodology and general discussion on erosion behaviour emphasised from the new, proposed models are presented.

Overview

The methodology section first describes both the bench tests and the CFD procedure. The technique of calibration using genetic algorithms is then introduced together with the erosion model functional selected. The results section reports the calibrations of the newly created models as well as the general flow features in the rigs, creating a plurality of impact characteristics that the genetic-algorithm-based calibration successfully overcomes. The response of the erosion models to important parameters is presented in the discussion section whose key findings are summarised in the conclusion.

METHODOLOGY

The erosion rate of a given massive target exposed to a given dispersed abrasive material was experimentally determined from bench testing. On the other hand, experimentally acquiring data about particles trajectories as they hit the target was a difficult task and CFD of binary flows was adopted for this purpose. It is established that state-of-the-art fluid mechanics computation is up for this task (Zhang et al., 2007). Eventually, experimental erosion data and numerical predictions of impacts fed into an inverse problem whose output was the set of parameters defining a phenomenological erosion model calibrated for this target/dispersed couple. The CFD simulations are used for collecting particle impact events on the target only and complement experimental data in this respect: there is no CFD prediction of erosion.

Experiments

Two configurations were investigated: erosion by semi-sharp Garfield sand (shape factor 0.7) of stainless steel in a pneumatic flow, and of aluminium in a slurry flow. The latter case was a difficult one to test the robustness of the calibration procedure as, first, the strong drag force from the carrier on

2

the particles induced significant perturbations of the particles trajectories as they approached the target, and second, the ductility of the material exhibited marked inhomogeneous erosion due to impact angle sensitivity.

Bench for Erosion of Stainless Steel by Garfield Sand Pneumatic Flow

The experimental apparatus for performing the erosion rate determination of stainless steel by a pneumatic flow loaded with Garfield sand consisted of an open-circuit round pipe wind tunnel. The wind tunnel had three main sections: an initial horizontal leg in which the dispersed phase falling through a side duct from a hopper mixed with the flow; a vertical test section to distribute the dispersed phase, and then a horizontal exhaust section to a cyclone and bag house for particle collection. The test rig was effectively the vertical round pipe leg, 102.5 mm in diameter, in which the Reynolds number developed was Re = 527,000. The sand size distribution is explained in the following Computations Section. The sand-to-carrier density ratio was 2240. Erosion was determined on the surface of a removable cross-flow cylinder. The cylindrical sample was positioned approximately 25 diameters downstream of the vertical leg entry. The cylinder diameter was 1/10th of the rig pipe diameter. The mid-line profile of the outer surface of the cylinder (black circle in Figure 1) was measured accurately, and the sample then placed in the wind tunnel and subjected to the gas/particle flow. The sample was removed, and its profile re-measured. By determining the difference in profiles before and after the experiment, the surface erosion velocity on the profile was calculated for a given cylinder angle β (defined in Figure 1). The sand capacity of the hopper provided the information on the amount of sand passed through the rig.

The profile of the cylindrical sample was measured by a purpose-built profile measuring apparatus, consisting of a collect chuck for holding the sample whose rotational position was controlled by a stepper motor connected to a computer. A Schaevitz gauge head allowed measurement of the surface to an accuracy of 3 μm and the stepper motor ensured rotational resolution of 0.45°. This ensured a lower relative uncertainty of a couple of percent on the erosion depths. Further details of the device are given elsewhere (Lester et al., 2010).

Bench for Erosion of Aluminium by Garfield Sand Slurry Flow

The slurry flow rig was made of a single vertical round pipe section, 52.6 mm in diameter. The water flow was measured by a Rosemount magnetic flowtube with 5% relative accuracy, translating into about 10% relative uncertainty in the erosion measurement (erosion is reckoned to exhibit a close-to-quadratic velocity dependency). The slurry flow was allowed to naturally develop in the vertical pipe for about 40 diameters before encountering the transversely placed cylinder test specimen obstructing 24% of the flow section. The slurry was returned to a mixing tank through flexible hose, sand was recycled. The Reynolds number developed in the pipe was 354,000. The sand size distribution is explained in the following Computations Section. The sand-to-carrier density ratio was 2.66.

Computations

CFD simulations of the experiments were carried out. The impacts of the particles on the target cylinder were recorded in terms of location, velocity magnitude and angle, and diameter of the projectile. The computations were performed in double-precision with ANSYS-CFX 14.0 and the ANSYS14 suite for pre-/post-processing.

The turbulent flow of constant-property fluid was modelled with the k-ω SST model and the sand particles were tracked as Lagrangian spherical parcels whose size followed the experimental distribution, Figure 2, and subject to Schiller-

Naumann drag, turbulent dispersion, virtual mass force and pressure gradient force.
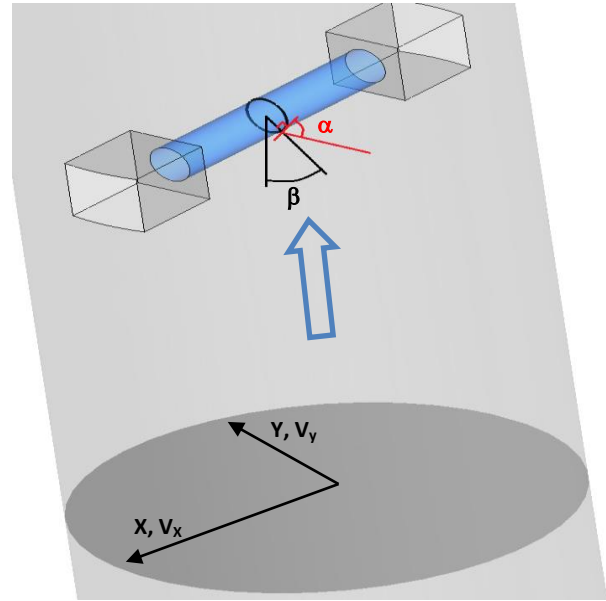

Figure 1: Coordinate system for surface of cylinder and rig cross-section.

The particle size is presented non-dimensionalised as a Stokes number:

$$St_d = \frac{\rho_d d^2 V}{18 \mu L} \qquad (1)$$

with μ and V the carrier dynamic viscosity and bulk velocity in the test section where the cylinder resides, d the particle diameter, ρ_d the sand density, and L the cylinder diameter.
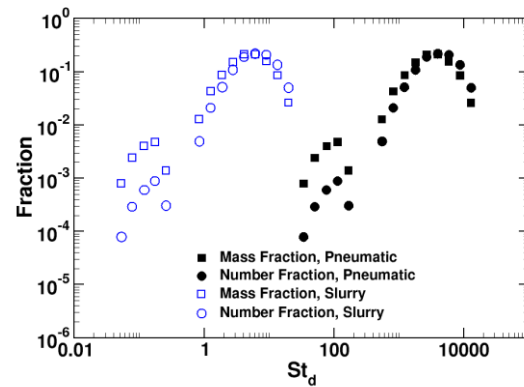

Figure 2: Mass-fraction-based size distribution of semi-sharp Garfield sand used in the erosion test, non-dimensionalised from bench operating conditions. 'Number Fraction' indicates the CFD Lagrangian parcels statistical distribution.

At the inlet, the flow velocity was prescribed with a turbulent profile (De Chant, 2005) with a 5% turbulence intensity and a viscosity ratio of 10. Walls were assumed numerically smooth. Particles entered the system at a prescribed speed (pneumatic bench) or in equilibrium with the flow (slurry bench). Restitution coefficient on the walls were set at 0.8 and 0.9 for the parallel and perpendicular components respectively (Humphrey, 1990). A Neumann outlet was imposed downstream. All transport equations were solved with second-order accurate schemes.

The mesh independency was assessed with a grid convergence index (Roache, 1994) of the order of a few percent. The grid convergence index can be interpreted as

3

commensurate, while generally lower, with the relative uncertainties associated with the numerical method. It was checked that the near wall regions were appropriately solved with a wall distance (y^+) mostly between 20 and 200 and a peak of eddy viscosity away from any surface by a minimum of five mesh elements. The mesh was made of a mixture of tetrahedral elements and prisms to accommodate both geometry and main flow direction. Skewness was kept under 0.5 and orthogonality above 0.6. The iteration convergence was also checked with insignificant changes when the residual tolerance was reduced by one order of magnitude. Conservation imbalances, including the parcels flux, were checked as virtually nil. Statistical independency of the Lagrangian solver was obtained with four million parcels launched.

Erosion Model Calibration

The calibration procedure involves the minimisation of a cost function that measures the difference between the experimental erosion profile on the mid-line of the cylinder and the predicted one using the erosion model fed with, on the one hand, the sand impact events on the target recorded by the CFD, and, on the other hand, a set of tuning parameters.

The erosion model chosen is from (Chen et al., 2004) extended with a diameter dependency function and has the form:

$$e = K v^n f(\alpha) \ \min\left(\frac{d}{d_c}, 1\right) \qquad (2)$$

with

$$f(\alpha) = (A\alpha^2 + B\alpha)_{\varphi > \alpha} + (X \cos \alpha^2 \sin W\alpha + Y \sin \alpha^2 + Z)_{\alpha > \varphi} \qquad (3)$$

α and v are the impact angle and velocity, respectively, $f(\alpha)$ is a purely empirical function attempting to capture the impact angular dependency, and e is the erosion ratio or mass of target material removed per unit mass of impacting dispersed material, such that the results can be made independent of the solid concentration.

The trailing diameter dependency follows the most common conclusions in the Literature Review: a linear increase in the magnitude of the effect on erosion, until a particle diameter critical value d_c beyond which this effect saturates. The method presented in this paper is conceptually compatible with future sophistication of this function. The set of tuning parameters $\{K, A, B, W, \ X, Y, Z, \varphi, n, d_c\} \subset \mathbb{R}$ are to be inversed by the optimisation algorithm.

The quadratic cost function is:

$$\Phi = \sum_{i=1}^{m} \left(\frac{P_i - R_i}{C_i}\right)^2 \qquad (4)$$

The sum is performed on m measurement points (here, the locations along the cylinder mid-line where the erosion profile is probed). R_i is the reference (bench test) erosion measurement at location i and P_i is the prediction counterpart from the erosion model fed with the CFD data and for a given, inexact set of tuning parameters. C_i is a normalisation variable, here taken as a constant commensurate to the overall order of magnitude of the observed erosion level. The calibration procedure relies on a standard genetic algorithm, `optim_ga` in `Scilab`, a single-objective algorithm with bound constraints (Baudin et al., 2010). The use of genetic algorithms is warranted because of the inexpensive evaluation of the objective function while allowing a thorough parameters space search. Except the size of the population and number of generations that were increased, the algorithm parameters were kept at their standard values and are summarized in Table 1.

Table 1: Genetic algorithm parameters.

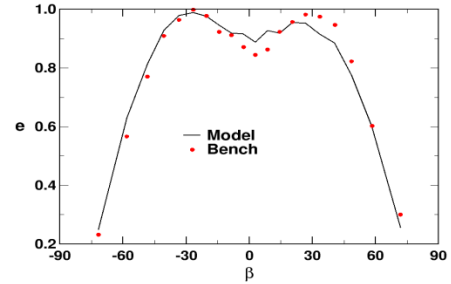| Parameter	Value
Generation	20
Population	200
Pressure	0.05
Cross-Over	0.7
Mutation	0.1
Couples	110

RESULT

Figure 3: Calibrated model on the experimental data. Stainless steel in a pneumatic flow.
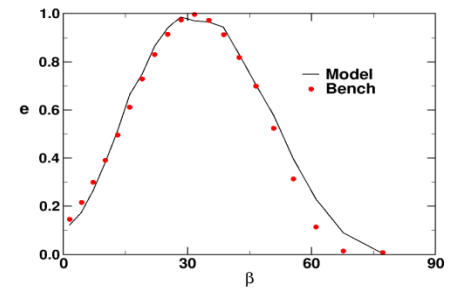

Figure 4: Calibrated model on the experimental data. Aluminium in a slurry flow.

The graphs showing how the genetic algorithm has eventually converged accurately on the experimental data while calibrating the underlying erosion models are provided in Figure 3 for the pneumatic flow eroding the stainless steel rod and in Figure 4 for the slurry eroding the aluminium rod. In particular, the models are calibrated well within the leading experimental uncertainties that are over 15% (vid. sup. Experiments & Computations Sections).

Figures 5 and 6 provide the location of the sand particles as well as their velocity in a cross-section plane one and a half pipe diameter upstream of the target as a function of their size, showing that the flux of particles is far from uniform in distribution and direction in the pneumatic rig. Figure 1 explains the local frame of reference on the cross-section to understand the axis of Figures 5 and 6. This is consistent with the lack of symmetry in the experimental erosion profile in Figure 3.

Similarly, the particle trajectories and impacts in the slurry rig are disorganised, this time, due to the perturbation by the fluid drag that goes around the target in the low-Stokes regime Figure 7.

For both models, Garfield pneumatic flow on stainless steel and Garfield slurry on aluminium, the threshold diameter d_c, Eq. 2, beyond which the erosion ratio reaches a plateau is consistent with what we reported in the literature review, that is, respectively, 0.373 mm and 0.157 mm.
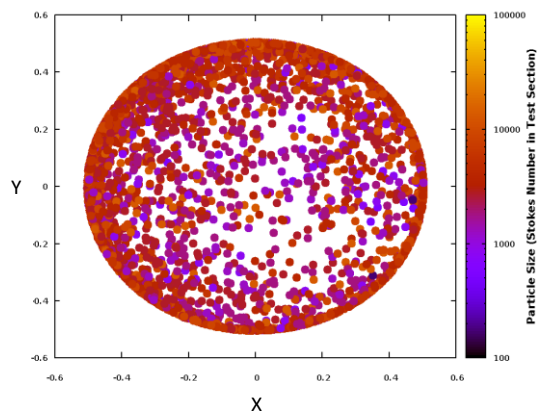
4

Figure 5: Particle trajectory locations in a cross-section plane one and a half diameter upstream of the target coloured by size non-dimensionalised as Eq. 1. Pneumatic case. Particle position coordinates X and Y are non-dimensionalised by test section diameter. Refer to Figure 1 for coordinates system definition.
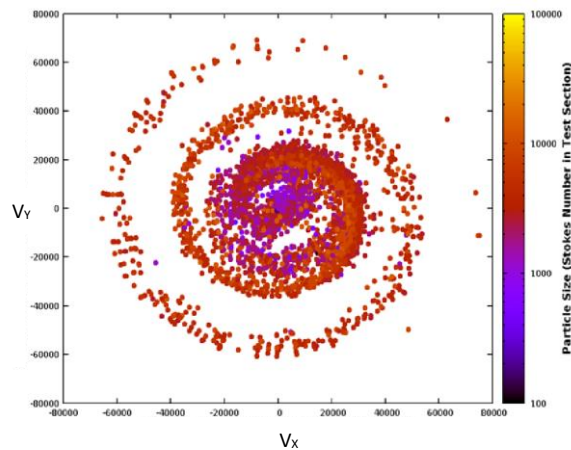

Figure 6: Hodograph of the particle velocities in a cross-section plane one and a half diameter upstream of the target coloured by size non-dimensionalised as Eq. 1. Pneumatic case. Particle velocity components V_X and V_Y are non-dimensionalised as pipe Reynolds number by flow conditions in the test section. Refer to Figure 1 for coordinates system definition.

Likewise, in the case of erosion of aluminium by Garfield slurry flow, the velocity exponent is recovered as 2.10 while it is 1.96 for stainless steel eroded by Garfield pneumatic flow. Both values are in accordance, within numerical and experimental uncertainties, with the concept that erosion is directly related to the impact kinetic energy of particles which should translate into a velocity exponent equal to two.

Other values of the erosion model parameters are not reported as they add little to the discussion.

DISCUSSION

The genetic algorithm allows one to extract implicit information from a raw set of data. There is, for example, no need to assume that the tracks are all parallel to each other following the axis of the flow to get the erosion angle response explicitly or that the flux of particles must be homogeneous and travelling at a uniform, assumed speed. In the same manner, an experimental particle size distribution can be used to capture erosion response to diameter even though the collected particle impacts and their associated contribution to erosion cannot be sorted in terms of particle diameter before feeding to the genetic algorithm. The accuracy obtained demonstrates that the genetic algorithm has no difficulty in calibrating the erosion models on the raw data. This is

remarkable as the aluminium cylinder is eroded by a slurry flow with particle trajectories highly perturbed by the carrier streamlines in an arbitrary manner. Likewise, the pneumatic case exhibits distributions in location and velocity of the particles approaching the target far from homogeneous.
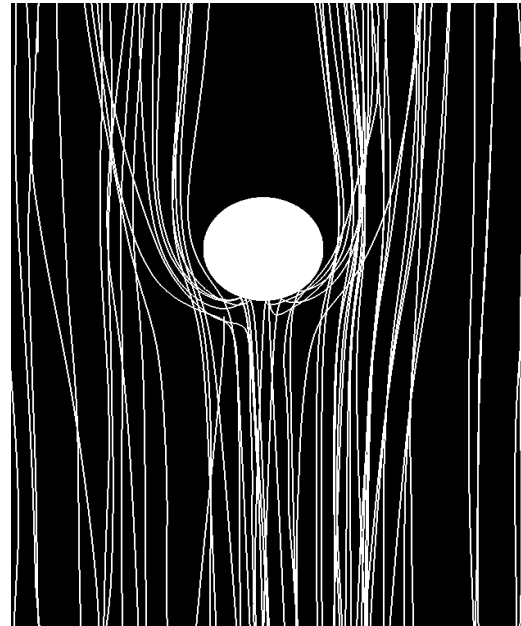

Figure 7: Sand trajectories. Slurry case.

From an engineering point of view, developing erosion models in a slurry rig transporting particles in the low Stokes regime has some advantages in terms of rigour and accuracy. The fact that the particle trajectories are controlled primarily by interactions with the fluid and not by interactions with the walls removes the uncertainties associated with restitution, which is a difficult issue to address when modelling particle transport and is the most appropriate candidate explanation for the inferior quality of the matching in the pneumatic bench compared to the slurry bench (Figure 3 versus Figure 4).

It is also remarkable that a single experiment at a defined flow rate is sufficient to recover a sensible velocity dependency: the genetic algorithm takes advantage of the slip velocities between particles and fluid to visit a range of impact velocities. Obviously, combining experiments with different bulk velocities would increase the constraint on the optimisation procedure in this respect.

The velocity dependency agrees with a kinetic energy argument. This is to be noted as materials of different ductility should differ from the kinetic interpretation and from each other in terms of velocity exponent, according to the state of the art. Should the present results be confirmed by more thorough studies, it would signify that the kinetic interpretation is the 'real physics' and that velocity exponents differing from two is mere artefact due to size erosion dependency not taken into account in models at the material level.

The threshold diameter that marks a transition in the erosion mechanism that makes it less sensitive to size is recovered in the range [100-500]µm and goes along with the understanding, still highly incomplete, of this aspect in the scientific community (see Literature Review).

The present study indicates therefore that genetic algorithms are suitable for erosion model calibration.

CONCLUSION

- The genetic algorithm is capable of directly treating the bench test raw data in which the erosion ratio is the result of the combination/undifferentiated

accumulation of impacts of particles with an arbitrary range of velocities, angles and diameters, to calibrate an erosion model;

- this paves the way to erosion model calibration in arbitrary configurations where particles speed, trajectory and size cannot be disentangled before inversion;

- in particular, it allows model development in the low-Stokes regime (slurry rig) which removes a large share of inaccuracy due to wall restitution.

- The paper extends the bench-test calibration of an established erosion model to account for particle diameter at the material level as a novelty. Conceptually, other parameters can be included and recovered by the genetic algorithm approach to account for additional yet unexplored physical properties.

- The extracted threshold diameter beyond which the mechanism of erosion becomes size-insensitive is consistent with what the literature reports while the velocity response of erosion is in accordance with the kinetic interpretation.

- The exact response to size seems to be far from understood and a simple mathematical function has been elected. There is no conceptual limitation for refinement if needs be and further investigations are warranted in order to provide a robust and reliable correction to erosion models for size dependency.

ACKNOWLEDGEMENT

REFERENCES

BAUDIN, M., COUVERT, V. and STEER, S., (2010), "Optimisation in Scilab", *Consortium Scilab*, Rocquencourt, France,.

CHEN, X., MCLAURY, B. S. and SHIRAZI, S. A., (2004), "Application and experimental validation of a computational fluid dynamics (CFD)-based erosion prediction model in elbows and plugged tees", *Comput. Fluids*, **33**, 1251-1272.

CLARK, H. M., (2002), "Particle velocity and size effects in laboratory slurry erosion measurements or... do you know what your Particles are doing?", *Trib. Int.*, **35**, 617-624.

CLARK, H. M. and HARTWICH, R. B., (2001), "A re-examination of the particle size effect in slurry erosion", *Wear*, **248**, 147-161.

DE CHANT, L. J., (2005), "The venerable 1/7th power law turbulent velocity profile: a classical nonlinear boundary value problem solution and its relationship to stochastic processes", *App. Math. Comput.*, **161**, 463-474.

DESALE, G. R., GANDHI, B. K., and JAIN, S. C., (2009), "Particle size effects on the slurry erosion of aluminium alloy AA 6063", *Wear*, **266**, 1066-1071.

DET NORSKE VERITAS, (2007), "*Recommended practice RP 0501 erosive wear in piping systems*".

ELFEKI, S. and TABAKOFF, W., (1987), "Erosion study of radial flow compressor with splitters", *Comput. Fluids*, **109**, 62-69.

FINNIE, I., (1960), "Erosion of surfaces by solid particles", *Wear*, **3**, 87-103.

HUMPHREY, J. A., (1990), "Fundamentals of fluid motion in erosion by solid particle impact", *Int. J. Heat Fluid Flow*, **11**, 170-195.

JORDAN, K., (1998), "Erosion in multiphase production of oil & gas", *Int. Corrosion Conf. Expo.*, San Diego, USA, March 22-27.

LAITONE, J. A., (1979), "Aerodynamic effects in the erosion process", *Wear*, **56**, 239-246.

LESTER, D. R., GRAHAM, L. A. and WU, J., (2010)., "High precision suspension erosion modelling", *Wear*, **269**, 449-457.

LYON, R. S., WONG, K. K. and CLARK, H. M., (1991), "On the particle size effect in slurry erosion", *Wear*, **149**, 55-71.

MCLAURY, B. S. and SHIRAZI, S. A., (1999), "Generalization of API RP 14E for erosive service in multiphase production", *SPE Annual Tech. Conf. Exhib.*, Houston, USA, , October 3-6.

ROACHE, P. J., (1994), "Perspective: a method for uniform reporting of grid refinement studies" *J. Fluids. Engng*, **116**, 405-413.

ROSENBERG, S. J., (1930), "The resistance of steels to abrasion by sand", *B. S. J. Res.*, **5**, 553-574.

SALAMA, M. M., (1998)a, "An alternative to API 14E erosional velocity limits for sand laden fluids", *Offshore Tech. Conf.*, Houston, USA, May 4-7.

SALAMA, M. M., (1998)b, "Sand production management", *Offshore Tech. Conf.*, Houston, USA, May 4 - 7.

SCHWEITZER, M. O. and HUMPHREY, J. A., (1988), "Note on the experimental measurement of particles embedded in one and two in-line tubes in a high speed gas stream", *Wear*, **126,** 211-218.

SOLNORDAL, C. B., WONG, C. Y., ZAMBERI, A., JADID, M. and JOHAR, Z., (2013), "Determination of erosion rate characteristic for particles with size distributions in the low-Stokes number range", *Wear*, **305**, 205-215.

STACK, M. M. and PUNGWIWAT, N., (1999), "Slurry erosion of metallics, polymers, and ceramics: particle size effects", *Mat. Sci. Tech.*, **15**, 337-344.

WALLACE, M. S., DEMPSTER, W. M., SCANLON, T., PETERS, J. and MCCULLOCH, S., (2004), "Prediction of impact erosion valves geometries", *Wear*, **256,** 927-936.

WONG, C. Y., BOULANGER, J. A. and SHORT, G., (2014), "Modelling the effect of particle size distribution in multiphase flows with computational fluid dynamics and physical erosion experiments", *Adv. Mat. Res.*, **891/892**, 1615-1620.

WONG, C. Y., SOLNORDAL, C. B., SWALLOW, A., and WU, J., (2013), "Experimental and computational modelling of solid particle Erosion in a pipe annular cavity", *Wear*, **303**, 109-129.

WONG, C. Y., SOLNORDAL, C. B., SWALLOW, A., WANG, S., GRAHAM, L. and WU, J., (2012), "Predicting the material loss around a hole due to sand erosion", *Wear*, **276/277**, 1-15.

ZHANG, Y., REUTERFORS, E. P., MCLAURY, B. S., SHIRAZI, S. A. and RYBICKI, E. F., (2007), "Comparison of computed and measured particle velocities and erosion in water and air flows", *Wear*, **263**, 330-338.